


RESEARCH ARTICLE



A new Kunitz-type snake toxin family associated with an original mode of interaction with the vasopressin 2 receptor

Laura Droctové¹ | Justyna Ciolek¹ | Christiane Mendre² | Amélia Chorfa² | Paola Huerta¹ | Chrystelle Carvalho¹ | Charlotte Guoin¹ | Manon Lancien¹ | Goran Stanajic-Petrovic¹ | Lorine Braco¹ | Guillaume Blanchet¹ | Gregory Upert¹ | Gregory De Pauw³ | Peggy Barbe¹ | Mathilde Keck¹ | Gilles Mourier¹ | Bernard Mouillac² | Servent Denis¹  | Ricardo C. Rodríguez de la Vega⁴ | Loïc Quinton³ | Nicolas Gilles¹

¹Département Médicaments et Technologies pour la Santé (DMTS), SIMoS, Université Paris Saclay, CEA, INRAE, Gif-sur-Yvette, France

²Institut de Génomique Fonctionnelle, Université de Montpellier, CNRS, INSERM, Montpellier, France

³Laboratory of Mass Spectrometry, MolSys Research Unit, University of Liège, Liège, Belgium

⁴Ecologie, Systematique Evolution, CNRS, AgroParisTech, Université Paris-Saclay, Orsay, France

Correspondence

Nicolas Gilles, Département Médicaments et Technologies pour la Santé (DMTS), SIMoS, Université Paris Saclay, CEA, INRAE, 91191 Gif-sur-Yvette, France.

Email: nicolas.gilles@cea.fr

Funding information

Commissariat à l'Énergie Atomique et aux Énergies Alternatives; Ligue Contre le Cancer

Background and Purpose: Venomous animals express numerous Kunitz-type peptides. The mambaquaretin-1 (MQ1) peptide identified from the *Dendroaspis angusticeps* venom is the most selective antagonist of the arginine-vasopressin V2 receptor (V2R) and the only unique Kunitz-type peptide active on a GPCR. We aimed to exploit other mamba venoms to enlarge the V2R-Kunitz peptide family and gain insight into the MQ1 molecular mode of action.

Experimental Approach: We used a bio-guided screening assay to identify novel MQs and placed them phylogenetically. MQs were produced by solid-phase peptide synthesis and characterized in vitro by binding and functional tests and in vivo by diuresis measurement in rats.

Key Results: Eight additional MQs were identified with nanomolar affinities for the V2R, all antagonists. MQs form a new subgroup in the Kunitz family, close to the V2R non-active dendrotoxins and to two V2R-active cobra toxins. Sequence comparison between active and non-active V2R Kunitz peptides highlighted five positions, among which four are involved in V2R interaction and belong to the two large MQ1 loops. We finally determined that eight positions, part of these two loops, interact with the V2R. The variant MQ1-K39A showed a higher affinity for the hV2R, but not for the rat V2R.

Conclusions and Implications: A new function and mode of action is associated with the Kunitz peptides. The number of MQ1 residues involved in V2R binding is large and may explain its absolute selectivity. MQ1-K39A represents the first step in the improvement of the MQ1 design from a medicinal perspective.

KEYWORDS

antagonist, Kunitz peptide, peptide sequencing, peptide synthesis, proteomics, snake venom, V2R

1 | INTRODUCTION

Animal venoms are rich in biologically active molecules, named toxins, displaying a wide variety of biological properties, including enzymes (proteases, phospholipases, nuclease etc.), enzyme inhibitors (as serine protease inhibitor) or ligands for membrane proteins like **ion channels** or **GPCRs**. In addition to their high affinity and selectivity for their various targets, animal toxins are highly stable thanks to a reticulated and rigid structure. Mamba snake venoms are mostly composed of two toxin scaffolds, the 3 finger-fold toxins (3FT) and the Kunitz-type toxins (Ainsworth et al., 2018). 3FT are active on ionic channels such as **calcium channels**, **ASIC channels** and **nicotinic ACh receptors**; on aminergic GPCRs; as well as on enzymes and **integrin** receptors (Blanchet et al., 2014; Kessler et al., 2017; Maïga et al., 2012). The Kunitz-type toxins are homologous to the bovine pancreatic trypsin inhibitor (**BPTI**) and have been initially described as inhibitors of various serine and cysteine proteases (Kunitz & Northrop, 1936). In the early 1980s, mamba Kunitz-type toxins known as **dendrotoxins** were identified with neurotoxic effects driven by their **potassium channel** blockade activities (Harvey, 2001). Later on, other Kunitz-type toxins were also described to inhibit **calcium channels** (Schweitz et al., 1994), the **vanilloid receptor 1** (Andreev et al., 2008) and ASIC channels (Bohlen et al., 2011). We recently assigned a new function to this structural family. The mambaquaretin-1 (MQ1) toxin isolated from the green mamba snake venom is the most selective antagonist of the type 2 arginine-vasopressin (**AVP**) human receptor (**hV2R**) so far described. It displays a nanomolar affinity for the hV2R and no effect on 156 other GPCRs (Ciolek et al., 2017). Up to now, it is the sole Kunitz peptide known to be active on a GPCR. We furthermore validated MQ1 as a therapeutic solution to hyponatremia and polycystic kidney diseases and as a diagnostic agent to detect V2R in vivo (Ciolek et al., 2017; Droctové et al., 2020).

Kunitz peptides are made of 56 to 60 residues in length and are characterized by a highly conserved $\alpha/\beta/\alpha$ conformation stabilized by three disulfide bridges (C1–C6/C2–C4/C3–C5). They also exhibit a strong intramolecular hydrophobic network (Huber et al., 1970). Their N-terminal extremity forms an α helix followed by a loop 1, which links to the first part of the antiparallel β sheet. The loop 2 connects the β sheet with the short C-terminal α helix. BPTI-like peptides interact with serine proteases via only 4 residues of its loop 1 and more particularly a dyad (residues 15 and 16) made of a basic residue followed by a glycine or alanine residue (Harper & Berger, 1967; Otlewski et al., 2001). Dendrotoxins, on the other hand, block the potassium channel **Kv1.1** predominantly with its lysine and an aliphatic residue positioned in the N-terminal extremity of the peptides (Gasparini et al., 1998). These two pharmacophores are diametrically opposed in the Kunitz structure (Figure 1) and are not present in MQ1. Consequently, MQ1 barely blocks Kv1.1 conductivity and inhibits trypsin activity at 25 μ M concentrations only (Ciolek et al., 2017). When restoring the pharmacophore of the dendrotoxin in MQ1 (MQ1-S3K, numbering according to the MQ1 sequence), potassium channel activity increases dramatically without affecting the V2R antagonism. When restoring the serine protease

What is already known

- The most selective V2R antagonist is a toxin extracted from the *Dendroaspis angusticeps* venom, the venom of other mamba species contains also Kunitz-type toxins.
- Kunitz peptides are known to interact with their molecular targets through small interaction surfaces.

What this study adds

- Kunitz-type toxins associate a new pharmacological activity with a new mode of interaction.

What is the clinical significance

- V2R is the unique validated therapeutic target for treating autosomal dominant polycystic kidney disease, an unmet therapeutic need. MQ1 is a promising therapeutic agent against this disease.

The MQ1/V2R interaction described here will help to improve MQ1 efficiency against this disease.

pharmacophore in MQ1 (MQ1-N15K + G16A), trypsin activity largely increases while the MQ1-V2R binding is disrupted (Ciolek et al., 2017).

In this study, we reassessed the diversity of mamba venoms by identifying eight new mambaquaretins (MQs), which form a distinct functional monophyletic group among the Kunitz-type peptides. These natural MQs altogether with synthetic variants brought new insights into MQ1 structure–activity relationships, highlighting the involvement of a large surface of the MQ1 structure in the V2R interaction, in sharp contrast to the way by which Kunitz peptides block potassium channels or inhibit serine proteases.

2 | METHODS

2.1 | MQs identification

Natural product studies are reported in compliance with the recommendations made by the British Journal of Pharmacology (Izzo et al., 2020). Venoms were fractionated as described (Ciolek et al., 2017). One gram of each *Dendroaspis* sp. venom (Latoxan, Valence, France) was separated into primary fractions by cation exchange LC (5 × 40 cm) on the resin Source 15S using a multi-step NaCl gradient at 20 ml·min⁻¹ on an Akta purifier (Pfizer, Quebec, Canada). The

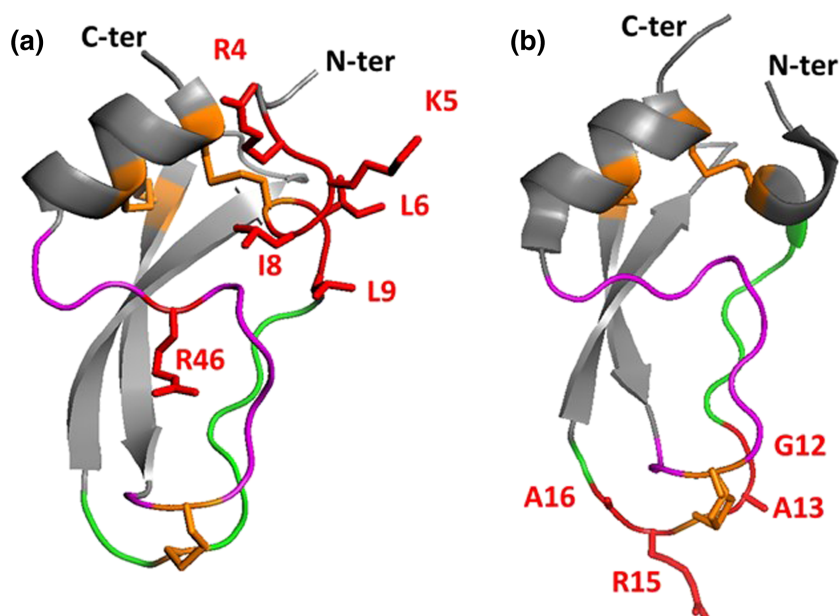


FIGURE 1 Pharmacophores of α -dendrotoxin and BPTI (in red sticks). Residues implicated in the binding of α -dendrotoxin (PDB: 1dtx) with Kv1.1 (Gasparini et al., 1998) (a) and BPTI (P13A variant, PDB: 1qlq) with serine proteases (Otlewski et al., 2001) (b). Loops are coloured in green (loop 1) and magenta (loop 2)

fractions were further purified by reverse-phase chromatography on a C18 Vydac preparative column (19.6 mm, 5 μ m, 25 cm), using a linear gradient from 0% to 100% acetonitrile in 0.1% trifluoroacetic acid over 100 min at a flow rate of 20 ml·min⁻¹. Analytical HPLC was finally performed on a C18 Vydac column (4.6 mm, 5 mm, 15 cm) using a gradient of 0.5% acetonitrile per min and a flow rate of 1 ml·min⁻¹. Protein concentrations were determined using the Bio-Rad protein assay with BSA as a standard. Toxin sequences were determined by mass analysis. Sequencing by in-source decay (ISD) MALDI-TOF was carried out with 15 μ g of each fraction treated with 2 μ l of 100 mM Tris(carboxyethyl)phosphine at 50°C and purified on a Zip-Tip C18 microcolumn. The matrix used for ISD experiments was 1,5-diaminonaphthalene (Accros). For peptide mass fingerprinting, 300 ng of purified toxins were reduced in 5 μ l of 50 mM NH₄HCO₃, pH 8, by 2 μ l of 250 mM DTT for 30 min at 56°C, followed by 2.2 μ l of 500 mM iodoacetamide for 1 h in the dark at room temperature. Mass analysis was made on a MALDI-TOF/TOF (rapiflex, Bruker Daltonics). Tandem MS experiments were performed using LIFT-TOF/TOF technology. Data were acquired with Flex Control 3.0. Resulting spectra were analysed with BioTools 3.2 and Sequence Editor 3.2 (Bruker Daltonics).

2.2 | Binding assay with radioligand

³H-AVP was purchased from PerkinElmer (Courtaboeuf, France). Binding experiments on self-prepared CHO cells overexpressing vasopressin hV2R subtype or HEK cells transfected with a plasmid coding for the rat V2R were performed on membrane preparations, in duplicate, as described (Ciolek et al., 2017; Droctové et al., 2020). Briefly, 1.5 nM ³H-AVP in a 100 μ l reaction mixture at room temperature in buffer composed of 50 mM Tris-HCl, pH 7.4, 10 mM MgCl₂ and 1 g·L⁻¹ BSA was incubated with

increasing concentrations of competitors for 3 h. Non-specific binding was measured in the presence of 1 μ M vasopressin. Incubation was stopped by filtration through 96 GF/C filter plates pre-incubated with 0.5% polyethylenimine. Twenty-five microlitres of Microscint O were added onto each dry filter and the radioactivity was quantified on a TopCount β counter with a 33% yield (PerkinElmer). We fitted competition binding data with the one-site/state inhibition mass action curve using KaleidaGraph (Synergy Software, Reading, PA, USA). IC₅₀ values were converted to K_i using 1 nM as K_d for hV2R and 1.4 nM for rV2R (Cornett & Dorsa, 1986) in the Cheng–Prusoff equation (Figure S6). Data represent independent experiments and are presented as the mean of pK_i \pm SEM.

2.3 | cAMP cell-based assay

The CHO cell line expressing hV2R (B. Mouillac, CNRS, Montpellier, France) was cultured at 37°C in 5% CO₂ in DMEM containing 10% FCS and 100 units·ml⁻¹ penicillin/100 μ g·ml⁻¹ streptomycin supplemented with 0.1 mM non-essential amino acids and 0.4 mg·ml⁻¹ geneticin. We seeded CHO cells (5,000 per well) into 96-well plates for cAMP quantification. For stimulation curves (EC₅₀ determinations), CHO-hV2R cells were stimulated by increasing AVP concentrations in the absence (control conditions) or in the presence of increasing competitor concentrations in a total 50 μ l volume incubation medium containing DMEM, 5% BSA and 0.1 mM RO201724 (cAMP-phosphodiesterase inhibitor). For competition curves, 1.77 nM AVP stimulated CHO-hV2R cells in the absence (control conditions) or presence of increasing competitor concentrations. Experiments lasted for 30 min at 37°C and were stopped by the addition of 25 μ l of lysis buffer from the cAMP Dynamic 2 kit (Cisbio International) containing cAMP labelled with acceptor entity

first, then by the addition of 25 μl of lysis buffer containing donor fluorophore-labelled antibody against cAMP (100 μl total volume per well, Cisbio International, PerkinElmer). The fluorophores elicited a FRET signal ($F\% = 100 \times [R_{\text{pos}} - R_{\text{neg}}]/R_{\text{neg}}$) with R_{pos} fluorescence ratio (665/620 nm) measured in wells incubated with both donor- and acceptor-labelled entities, and R_{neg} being the same ratio for the negative control with donor fluorophore-labelled antibody only. This signal was then transformed into cAMP concentration in wells using a calibration curve. Activation/inhibition curves were plotted to the log of AVP concentrations and fitted to the Hill equation to extract the EC_{50}/IC_{50} values using GraphPad Prism software. The corresponding Arunlakshana-Schild plots allowed to determine pA_2 from the Schild equation. Experiments were done in triplicate. Data are presented as mean \pm SEM.

2.4 | In vivo experiments

Animal studies are reported in compliance with the ARRIVE guidelines (Percie du Sert et al., 2020) and with the recommendations made by the *British Journal of Pharmacology* (Lilley et al., 2020). The CEA animal experiment ethics committee approved the use of animals and experimental protocols (reference: APAFIS#1496-2015082111349702 v1). Six-week-old male Sprague-Dawley rats (RRID:RGD_70508) were obtained from Janvier Labs (Le Genest-Saint-Isle, France) and hosted in CEA Saclay animal facilities under stable and controlled conditions of temperature and pressure. Animals had free access to a standard rodent diet and to tap water. Metabolic cages were purchased from Tecniplast (Buguggiate, Italy). After 3 days in metabolic cages for habituation, rats were intraperitoneally injected with 0.5 $\text{ml}\cdot\text{kg}^{-1}$ of the toxin or vehicle dissolved in 0.9% NaCl solution. Urine outputs were collected 24 h post-injection and weighed. Animal weight, food and water intakes were also measured for control. Urinary pH was measured using a pH-meter SevenEasy™ (Mettler Toledo, Viroflay, France). Urinary osmolality was measured using a Type 13 automatic osmometer (Roebbling, Berlin, Germany). Urinary flow (UF) and Osmole excretion were reported to animal weight to avoid bias. $UF = \text{urinary volume}/(\text{time} \times \text{body weight})$. $\text{Osmole excretion} = (\text{urinary osmolality} \times \text{urinary volume})/(\text{time} \times \text{body weight})$.

2.5 | Peptide production

All the peptides were synthesized on a Prelude synthesizer (Protein Technologies®, Tucson, AZ, USA), purified and folded according to the method already described (Ciolek et al., 2017). Briefly, the solid-phase synthesis using an Fmoc strategy was done on 25 μmol of ChemMatrix®, peptide cleavage and purification. Linear peptides were folded in the presence of oxidized and reduced GSH (1 mM) and glycerol 20% (K10A) or guanidine 0.5 M (MQ2) in Tris buffer at pH 8 overnight at room temperature. All the other peptides were folded in the presence of oxidized and reduced cysteine (1 and 0.1 mM, respectively), in HEPES 100 mM at pH 7.5 (R44A, MQ4, MQ5, MQ6,

B4ESA3, C1IC51, D5J9Q8, F8J2F6 and Q5ZPJ7) and acetonitrile 20% (F18A, E7FL11 and P19859) or guanidine 0.5 M (MQ3, N-ter, N&C-ter, N6E, F21A, S24G, Q25A, K26A, K26E, K29A, H31F, V9S, N15A, F18A, S19A, T34F, K39A, K39E, K39W, N41A and S46R) or in Tris at pH 7.2 and guanidine 0.5 M (F17A and K10E), overnight at room temperature.

2.6 | Phylogenetic reconstruction

We used mafft v7.388 -auto option 4 to align eight MQs with 40 dendrotoxin full mature sequences from VenomZone (<https://venomzone.expasy.org/>) and three bovine protease inhibitors with the Kunitz fold included as outgroup (UniProt IDs: P00974, P00975 and P04815). With this multi-sequence alignment, we obtained a maximum likelihood (ML) tree with RAxML Version 8.2.7.5 under the PROTGAMMAJTT substitution model and the rapid hill climbing option (-f d). We calculate 15,000,000 trees with MrBayes v3.2.6 in three independent runs with four chains each under the JTT substitution model and rates = invgamma. We merged the 1000 trees with the best posteriors from each run and annotated the branches of the ML tree with RAxML -b option.

2.7 | Statistical analysis

The data and statistical analysis comply with the recommendations of the *British Journal of Pharmacology* on experimental design and analysis in pharmacology (Curtis et al., 2018). All statistical tests were performed with KaleidaGraph (Synergy Software). Multiple group comparisons were performed using a one-way ANOVA with post hoc test according to Dunnett. $P < 0.05$ was considered statistically significant. Values are expressed as means \pm SEM.

2.8 | Materials

Unless mentioned otherwise, all chemicals were from Sigma-Aldrich. AVP was from Bachem (Bubendorf, Switzerland), ^3H -AVP was from PerkinElmer (Courtaboeuf, France). Fmoc-amino acids, Fmoc-pseudoproline dipeptides and 2-(6-chloro-1-*H*-benzotriazole-1-yl)-1,1,3,3,-tetramethylammonium hexafluorophosphate (HCTU) were from Activotec (Cambridge, UK). The cAMP assay kit was from Cisbio (Marcoule, France). Cy5.5-DBCO and AFDye-488-DBCO were from Click Chemistry Tools (Scottsdale, AZ 85260, USA).

2.9 | Nomenclature of targets and ligands

Key protein targets and ligands in this article are hyperlinked to corresponding entries in <http://www.guidetopharmacology.org> and are permanently archived in the Concise Guide to PHARMACOLOGY 2021/22.

3 | RESULTS

3.1 | Mamba venoms, a source of V2R inhibitory toxins

Mambas (genus *Dendroaspis*) are venomous African Elapidae snakes, whose bites are often deadly without proper medical treatment. They live throughout sub-Saharan Africa in savannas and in tropical rain forest (Ainsworth et al., 2018). MQ1 was discovered in the *Dendroaspis angusticeps* (Da) venom by function-based screening (Ciolek et al., 2017). The same strategy was applied to three other mamba venoms (Figure 2). One gram of each *Dendroaspis polylepis* (Dp), *Dendroaspis jamesoni* (Dj) and *Dendroaspis viridis* (Dv) venoms were firstly fractionated by strong cation exchange LC (Figure 2a–c). Seven fractions (DpS, DpL, DjKN, DvC, DvG, DvK and DvL) inhibited tritiated vasopressin ($^3\text{H-AVP}$) binding on the human V2R stably expressed in a CHO cell line. These fractions were submitted to reverse-phase LC (Figure S1) to isolate DvGB (MQ2), DpSH (MQ3), DvKN (MQ4), DjKN (MQ5), DvLM (MQ6) and DvCK (MQ9) containing one toxin each fully sequenced by mass fragmentation strategies (Figure S2). The DpLK fraction contains two peptides, one previously described as DTX-B (Strydom & Joubert, 1981), which we refer to as MQ7, and a novel homologue with the A27S substitution (MQ8). The list of the active fractions, their masses and number of disulfide bridges, as well as their proportions in the venom are summarized in Table S1. Synthetic analogues of MQ2 to MQ6 were produced by solid-phase chemical synthesis (Figure S3). We succeeded in the synthesis of the linear forms of the three MQ7, MQ8 and MQ9 but failed in their oxidation steps. Consequently, their pharmacological characterizations were limited by the availability of natural products found in the venoms. In addition, MQ7 and MQ8 could not be separated from each other; thus, we characterized the effects of the MQ7/8 mix (DpLK fraction).

Binding competition experiments on hV2R showed that these novel MQs inhibit $^3\text{H-AVP}$ binding with affinities in the 1–100 nM range (Figure 2d and Table 1). Moreover, MQs dose-dependently inhibited AVP-induced cAMP production measured on a CHO cell line stably expressing hV2R (Figure 2e and Table 1), highlighting their

Binding competition experiments on hV2R showed that these novel MQs inhibit $^3\text{H-AVP}$ binding with affinities in the 1–100 nM range (Figure 2d and Table 1). Moreover, MQs dose-dependently inhibited AVP-induced cAMP production measured on a CHO cell line stably expressing hV2R (Figure 2e and Table 1), highlighting their

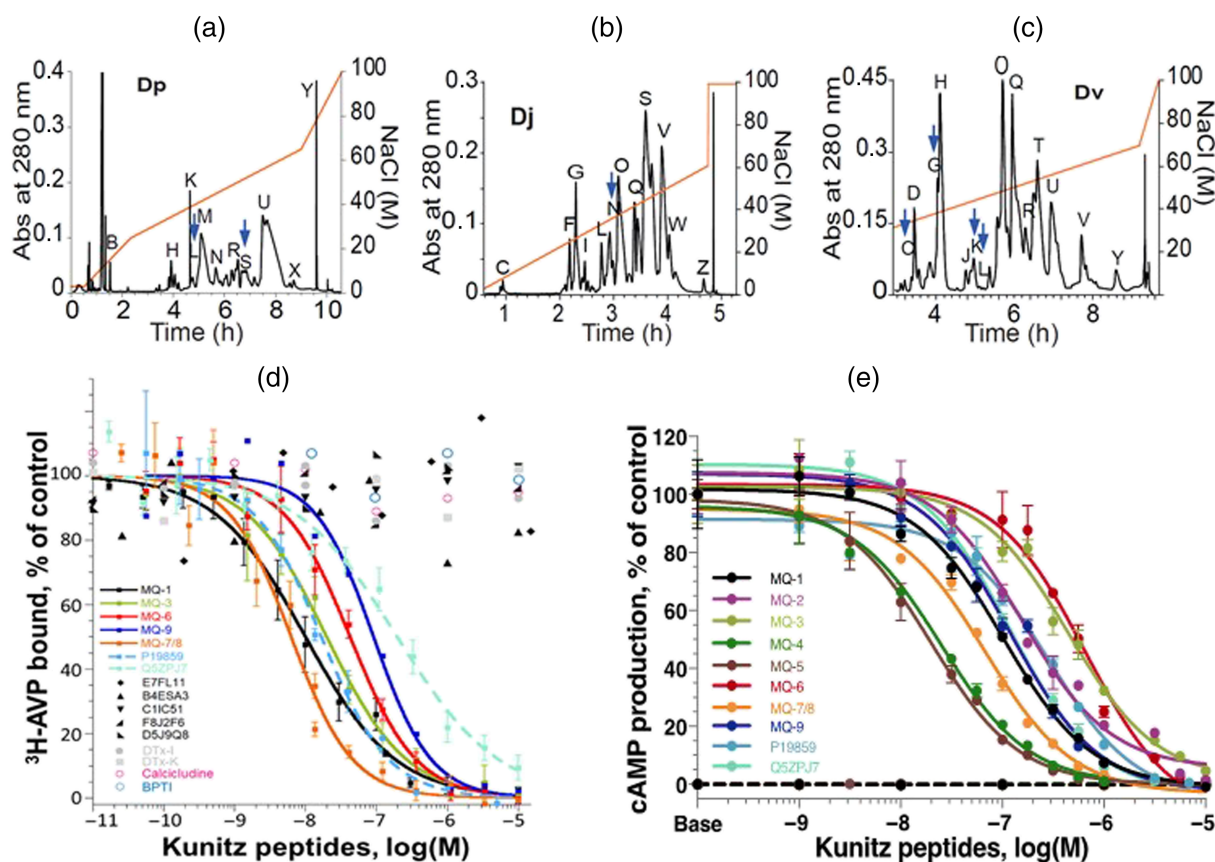


FIGURE 2 Identification and characterization of the MQs. Strong cationic exchange chromatography of Dp (a), Dj (b) and Dv (c). Blue arrows indicate active fractions on hV2R able to inhibit more than 50% of $^3\text{H-AVP}$ binding. (d) Binding of $^3\text{H-AVP}$ on hV2R in the presence of MQs (coloured squares; for a comparison of the complete set of toxins, see Table S2), P19859 and Q5ZPJ7 (blue dashed lines), Dtx-I (grey dots), Dtx-K (grey squares), calcicludine (pink open circle), BPTI (light blue open circle) or five other non-active Kunitz peptides (black symbols). α -DTX, MQ2, MQ4 and MQ5 curves are not shown for clarity. (e) Toxin antagonist effect on cAMP production induced by 1.77 nM of AVP on V2R (same colour code than for panel d). Dotted line corresponds to cAMP production with toxins in the absence of AVP

TABLE 1 Pharmacological properties of the V2R toxins

	Binding					AVP-induced cAMP inhibition					
	K _i (nM)	Ratio K _i	pK _i	SEM	n	IC ₅₀ (nM)	SEM	Ratio IC ₅₀	nH	n	IC ₅₀ versus K _i
MQ1	5.02	-	8.44	0.1	25	94	8	1	1.08	16	19
MQ2	8.16	1.6	8.17	0.15	4	224	62	2.4	1.05	3	28
MQ3	13.3	2.6	7.92	0.14	4	453*	75	4.8	0.92	3	34
MQ4	7.34	1.5	8.27	0.21	5	26	7	0.3	0.91	3	3.5
MQ5	3.50	0.7	8.58	0.3	4	21	9	0.2	0.95	5	6
MQ6	21.5*	4.3	7.60	0.1	5	574*	186	6.1	1.19	3	27
MQ7-8	3.14	0.6	8.53	ND	2	58	17	0.6	0.99	3	18
MQ9	45.1*	9.0	7.35	ND	2	111	30	1.2	1.15	3	2.5
P19859	7.87	1.6	7.93	0.08	4	208	51	2.2	0.94	3	6.5
Q5ZPJ7	112*	22.2	6.97	0.08	4	138	1.5	23	1.16	3	1.2
E7FL11	>>1000		<<5		2	ND					
B4ESA3	>>1000		<<5		2	ND					
C1IC51	>>1000		<<5		2	ND					
D5J9Q8	>>1000		<<5		2	ND					
F8J2F6	>>1000		<<5		2	ND					
D-DTx	>>1000		<<5		2	ND					
DTx-K	>>1000		<<5		2	ND					
α-DTx	>>1000		<<5		2	ND					
DTx-I	>>1000		<<5		2	ND					
Calci	>>1000		<<5		2	ND					
BPTI	>>1000		<<5		2	ND					

Note: The statistical significance was assessed for binding by a one-way ANOVA with post hoc test according to Dunnett in comparison with MQ1. Means represent 2 to 25 independent experiments.

Abbreviations: BPTI, bovine pancreatic trypsin inhibitor; Calci, calcicludine; MQ7-8, MQ7 + MQ8; ND, not done.

*P < 0.05.

antagonist activity (MQs never induced a cAMP production by themselves). When comparing affinities (K_i) and potencies (IC₅₀) of tested toxins, we obtained various ratios. MQ1, MQ2, MQ3, MQ6 and MQ7/8 gave similar ratios between 18 and 34. MQ5, MQ9, P19859 and Q5ZPJ7 gave much lower ratios between 1.2 and 6 (Table 1). The second group of toxins displayed relatively better potency in inhibiting cAMP production induced by vasopressin than inhibiting ³H-vasopressin in our binding study. One may think that these two groups of toxins interact differently with the hV2R. This hypothesis is unlikely. Indeed, the percentage of sequence identity between all these toxins strongly suggest a very similar interaction with the V2R. Another explanation may be link to the experimental conditions used here. Binding studies were done under equilibrium conditions with an incubation time of 3 h, while functional tests were performed under 30 min of incubation time. Then, the second group of toxins may have a faster K_{on} than the first one, allowing it to better block vasopressin activation compared with vasopressin binding. The in vivo diuretic effects of the synthetic MQs (MQ1-MQ6) were investigated in Sprague-Dawley male rats after a single i.p. injection. Control rats urinated an average of 43 ml·day⁻¹·kg⁻¹ BW. MQ1-5 (30 nmol·kg⁻¹ BW) increased diuresis by 6.5-fold without any loss of

electrolytes (Table 2). MQ6, displaying a lower affinity for V2R and a lower potency to inhibit cAMP production in vitro, was tested at 100 and 300 nmol·kg⁻¹ BW, and a twofold increase in diuresis at the highest dose was observed. Irrespective of the MQ tested or the dose used, urine osmolality variation is inversely proportional to aquaresis modification (Table 2), demonstrating a pure aquaretic effect of the MQs.

3.2 | MQs form a distinct group of Kunitz-type snake toxins

Amino acid sequences of Kunitz peptides were aligned according to MQ1 with representative sequences of dendrotoxins and three BPTI sequences (P00974, P00975 and P04815; Figure 3a). This alignment was used to reconstruct the phylogenetic relationships of Kunitz-type snake toxins. The phylogram showed that all nine MQs constitute a well-supported monophyletic group, sister to ion-channel modulators isolated from mambas (so-called dendrotoxins). MQs are organized into two subgroups: MQ1 to MQ6 are very closely related to each other, whereas MQ7 to MQ9 are more divergent (Figure 3b, red

TABLE 2 In vivo properties of V2R toxins

	n	Dose (nmol·kg ⁻¹ BW)	24 h diuresis (ml·kg ⁻¹ ·h ⁻¹)	SEM	Osmolality (mOsm·kg ⁻¹ H ₂ O)	SEM	Osmoles excretion (μOsmol·h ⁻¹ ·kg ⁻¹ BW)	SEM
Control	6		1.79	0.17	1279	200	2137	200
MQ1	9	30	11.8*	0.83	227*	10	2728	70
MQ2	6	30	9.79*	0.83	326*	70	2940	300
MQ3	6	30	8.17*	0.83	289*	30	2277	100
MQ4	5	30	15.4*	2.1	209*	40	2826	90
MQ5	6	30	11.0*	1.7	240*	20	2592	400
MQ6	3	300	3.38*	0.83	765*	100	2360	200
P19859	3	100	2.88*	0.42	779*	30	2215	400
Q5ZPJ7	3	30	3.92*	0.42	726*	75	2712	165

Note: Statistical test was assessed by a one-way ANOVA with post hoc test according to Dunnett in comparison with control.

Abbreviation: BW, body weight.

*P < 0.05.

background). MQ8 is a natural variant of the dendro-B (P00983, named here MQ7), and is a weak trypsin inhibitor (Strydom & Joubert, 1981). Both diverge from MQ1 by 19 mutations. MQ9 is the most original sequence with 21 mutations compared with MQ1 and a one residue shorter loop 1 (Figure 3a). All MQs are a sister group to a branch composed of seven dendrotoxins (Figure 3b, blue background). The peptides DTX-R55 (Q7LZS8) and DTX-E (P00984) have never been characterized and are probably active on serine proteases as they possess the dyad Lys15–Ala16. The five other dendrotoxins are potassium and calcium channel inhibitors, which are not active on V2R up to 10 μM (Figure 2d).

The next group is composed of two cobra toxins (Figure 3b, green background). P19859 is an uncharacterized toxin from the Indian cobra *Naja naja* (Shafqat et al., 1990). Q5ZPJ7 is a weak **chymotrypsin** inhibitor from the Chinese cobra *Naja atra* (Zhou et al., 2004). The synthetic versions of P19859 and Q5ZPJ7 (Figure S4) bind V2R (Figure 2d) and antagonize cAMP production (Figure 2e and Table 1) with K_i and K_{inact} equivalent to those of other MQs. Injected in rats, both cobra toxins raise diuresis (twofold increase) with a concomitant decrease of urine osmolality, demonstrating an aquaretic effect (Table 2). The other sequences used to build the phylogram belong for the most part to viper or Australian snakes. Among them, we checked the activity of five selected toxins (E7FL11, B4ESA3, D5J9Q8, F8J2F6 and C11C51; Figure S4) distributed all along the dendrogram and having a dyad composition compatible with V2R activity (Asn15–Gly16, Asn15–Ala16 or His15–Gly16). None of them were active on V2R up to 10 μM (Figure 1d).

The nine MQs constitute a new phylogenic Kunitz group associated with a V2R activity. The comparison between the 11 V2R-active toxin sequences and the non-active V2R Kunitz peptides highlighted five positions that might play positive roles in binding to the V2R (Figures 3a and S5). The positions 17, 28 and 44 are strictly conserved in V2R-active Kunitz and highly variable in non-active V2R Kunitz. The position 34 is occupied by a threonine residue in 10 toxins and by an asparagine in one. It is highly variable in non-active V2R Kunitz.

Finally, the position 10 is basic (Lys) or neutral (Ala, Ser) in V2R-active Kunitz whereas it is mostly acidic in other Kunitz groups (Figures 3a and S5).

3.3 | MQ1 uses its two large loops to bind V2R

To characterize the importance of the five positions described above for hV2R interaction, we synthesized the variants K10E, F17A, N28A, T34A and R44E. We could not obtain the folded N28A variant. The five remaining variants induced a loss of 20-fold to 1340-fold in binding affinity (Figure 4 and Table S2). Interestingly, they all belong to the MQ1 loops 1 and 2 (Figure 3a). We expanded our analysis to other neighbouring positions excluding structural (Cys, Ala, Gly, Pro) and buried positions (Tyr22, Tyr23, Phe33, Tyr35). We found that residues Val9 and Phe18 but not Ser19, Asn41 or Ser46 are in interaction with the V2R. Surprisingly, whereas the variants K39E and K39W never modified MQ1 affinity on hV2R, the K39A improved it by almost 9 times (Figure 4 and Table S2). We confirmed here previously demonstrated data showing that the N- and C-terminal extremities (Figure 4) are not involved in the binding process of MQ1 (Ciolek et al., 2017). Finally, the structured part of the toxin defined by residues implied in α helix or β sheets never participate to V2R binding as the variants N6E, F21A, S24G, Q25A, K26A, K26E, K29A and H31F displayed the same affinities for hV2R as MQ1.

3.4 | MQ1-K39A is specific for human V2R

We expanded the study of the variant MQ1-K39A, because the substitution of a lysine residue by alanine significantly improved MQ1 affinity for hV2R. MQ1 and MQ1-K39A shifted to the right of the AVP-dependent cAMP production on CHO cell lines expressing the hV2R (Figure 5a,b). Arunlakshana–Schild plots show a purely competitive behaviour between vasopressin and the toxins, and IC₅₀

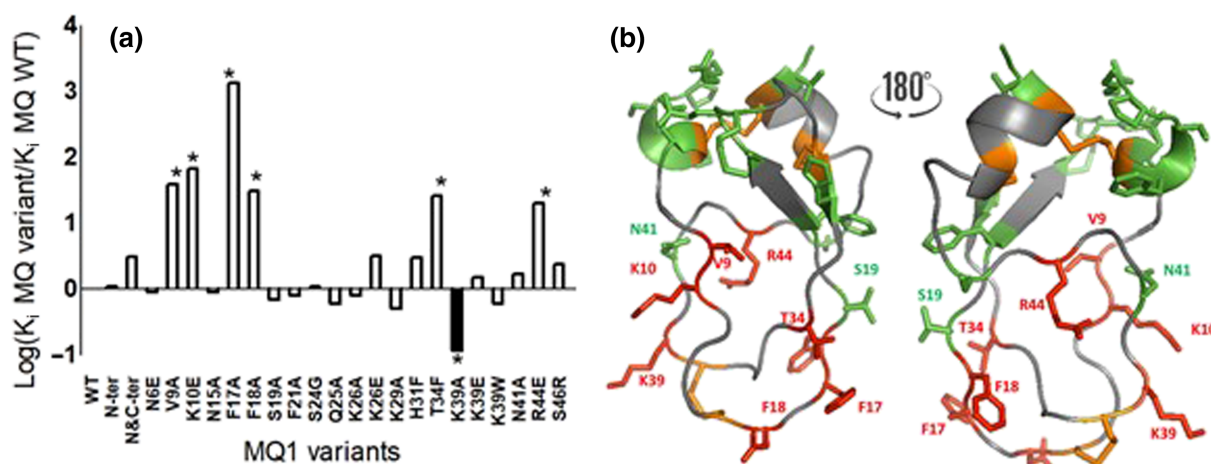


FIGURE 4 Structure–activity relationships of MQ1. (a) Affinities ratios of MQ1 variants. * $P < 0.05$. N-ter: MQ1 without the four first residues RPSF. N&C-ter: MQ1 without the four first residues RPSF without the two last residues GV and with the terminal cysteine residue being amidated. (b) Front and back sticky representation of tested MQ1 positions (PDB: 5m4v). Variants that influence (red) or not (green) on MQ1 affinity for hV2R are shown

4 | DISCUSSION

In this study, we enlarge the Kunitz-type toxin family active on the V2 vasopressin receptor through identification and characterization of novel mamba and cobra V2R antagonist ligands. Thanks to screening experiments and phylogenetic analysis, these structured ligands enable us to understand a new molecular mechanism for their interaction with the V2R.

Mamba (African species) and cobra (Asian species) are two evolutionary-distant and geographically distant snakes. The presence of a cobra toxin group also active on V2R suggests either (1) independently derived V2R activity of Kunitz toxins from cobras and mambas or (2) conserved V2R activity due to shared ancestry (ion-channel blockade of dendrotoxins would be the derived activity). The presence of toxins active on V2R in various Elapid snake venoms suggests an important role of these toxins for snakes' survival. However, whether or not the V2R activity is their selected function in the ecological context of venom use remains to be established. We note that as long as victim has access to water, blockage of V2R should not be toxic at all. In any case, the screening of new targets, like GPCRs, allowed us the discovery of new group of toxins with a strong activity on a pharmaceutically relevant receptor, highlighting the extraordinary diversity of animal toxins present in venoms that remains largely underexplored.

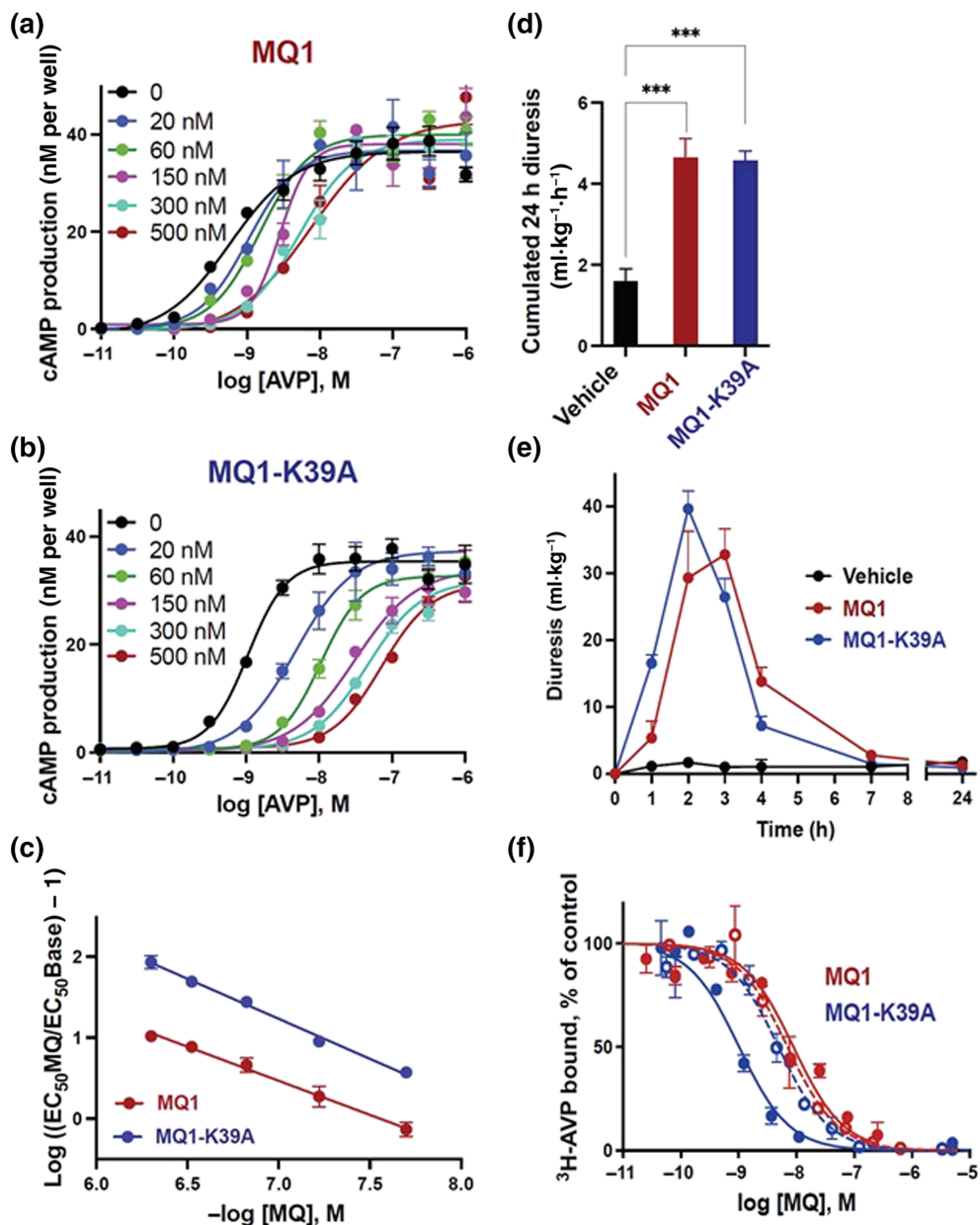
The identification of a new monophyletic group in the Kunitz peptide family constituted an opportunity to better understand the molecular mechanisms supporting the pharmacological properties of these toxins. The natural SAR highlighted the importance of the two MQ1 major loops in V2R binding, which was confirmed by an extended number of characterized MQ1 variants. MQ1 shows a new strategy to bind to its target compared with α -DTX (Figure 1, Gasparini et al., 1998) and BPTI (Figure 1, Kawamura et al., 2011). Indeed, whereas α -DTX uses its structured part to block Kv1.1 and BPTI its loop 1 to inhibit serine proteases, MQ1 exploited its two

major loops and engages more positions in its interaction with V2R. The pharmacophore defined by numerous amino acids positioned in loop 1 (9 to 18) and loop 2 (34, 39 and 44) may be at the origin of the absolute selectivity of MQ1 for the V2R.

MQ1 displays the same nanomolar affinity for rat and human V2R (Droctové et al., 2020) but no interaction with V1a, V1b or OT receptors (Ciolek et al., 2017). Figure 6 shows a sequence alignment between the three external loops (ELs) of the vasopressin-sensitive receptors. When comparing these five receptor sequences, nine positions appeared as V2R specific versus V1Rs and OTR. Three are acidic residues: D103 (numbering according to the hV2R) in ECL1, E198 in ECL2 and E299 in ECL3, and six are non-polar residues, all in ECL3. The three MQ1 basic residues implied in V2R binding (K10, K39, R44) and the three V2R-specific acidic residues just described point to a charge complementarity between the two partners. In addition to these nine specific positions, differences in loop length may play a role in the MQ1 selectivity. OTR ECL2 is shorter by two residues compared with V2R whereas the V1Rs ECL3 ones are longer by three residues. Even if extensive structure–activity relationships should be done to validate these hypotheses, these data describe the implication of important residues covering a large surface of contact for MQ1, which appear to be in coherence with a possible implication of the three V2R ECLs in the complex MQ1/V2R formation.

MQ1-K39A showed an interesting 14-fold higher specificity for hV2R versus rV2R. Too many mutations exist between rat and human V2R sequences to propose any hypothesis, but MQ1-K39A represent a new tool to gain insights into its mode of action. This specificity shows that these toxins can display different affinities for the human and the rat V2R. The fact that MQ6 and P19859 are much less efficient at increasing rat diuresis compared with MQ1, despite similar affinities for the human V2R, may come from a lower affinity for the rat V2R. Otherwise, we may think that Q5ZPJ7 could display higher affinity for the rat than the human receptor regarding its in vivo effect

FIGURE 5 In vitro and in vivo characterization of MQ1-K39A. Competitive inhibition of AVP-induced cAMP production in stable CHO-hV2R by MQ1 (a) and MQ1-K39A (b). (c) Corresponding Arunlakshana–Schild plots. Schild representations are plotted as mean \pm SEM, $n = 4$ (MQ1, red) or 5 (MQ1-K39A, blue). (d) Cumulated 24 h rat diuresis after administration by i.p. route. Black: Vehicle. Red: 3 nmol·kg⁻¹ BW of MQ1, blue: 3 nmol·kg⁻¹ BW of MQ1-K39A, $n = 6$. (e) Rat diuresis versus time post-injection at 3 nmol·kg⁻¹ BW. Same colour code. (f) Representative binding competition curves of MQ1 (red) and MQ1-K39A (blue) on hV2R (full line) and rV2R (dashed line, $n = 3$), expressed as mean \pm SEM



	ECL1 103	ECL2 198	ECL3 292 299 306 310
hV2R	WKAT DR FRGPD	QRNVEGGSGVTD WC ACFA EP WGRR T	VQL WA AWD PE APL-EGAP FV --LLMLL
rV2R	WDAT DR FHGPD	QRDVGNGSGVFD CA WARFA EP WGLRA	VQL WA AWD PE APL-EER PPV --LLMLL
hV1aR	WDITYRFRGPD	MIEVNNVT K ARD C WATFIQ P WGSRA	IQMWSVWD P MSV W TESENPTITITALL
hV1bR	WDITYRFRGPD	LREVIQSGSVLDC WA DFG F PWGPRA	VQMWSVWD K NA PE DE D ST N VAF T ISMLL
hOT	WDITFRFRGPD	LRE V AD--GV F DC WA VFIQ P WGPKA	VQMWSVWD A NA PK -EASAFI--IVMLL

FIGURE 6 Sequence analysis of vasopressin-sensitive receptors. In bold, residues that are identical between rat (r) and human (h) V2Rs but variable in hV1aR, hV1bR and hOT. Red: Acidic residues. Orange: Non-polar residues. ECL: Extracellular loop

and its affinity for the human V2R. Blocking the V2R is a validated therapeutic line for several pathologies like the autosomal dominant polycystic kidney disease (Juul et al., 2014). Improving the in vivo activity of MQ1 is important to develop a new therapeutic option for V2R-related diseases. This work presents an upgraded version of MQ1.

The Kunitz structure is active on three major classes of molecular targets: enzymes, channels and receptors. It is a rare situation for animal toxins where each active compound is linked in great part to only one activity. Only the 3FT family, exclusively produced by snakes, target these three classes of proteins that are enzymes (serine proteases for BPTI, ACh esterase for fasciculins; Bourne et al., 1995), ion

channels (Kv1.1 for the dendrotoxins, ASIC channel for the mambalgins; Sun et al., 2018) and GPCRs (V2R for MQ1, **muscarinic** receptors, and **adrenoceptors** for aminergic toxins; Blanchet et al., 2017; Quinton et al., 2010; Rouget et al., 2010). The 3FT toxins are composed of three loops called fingers linked by a structured part rich in disulfide bridges (Fruchart-Gaillard et al., 2012). 3FT always use their fingers to interact with their targets. The fasciculins and the mambalgins use their first and second fingers whereas the MT7 uses all of its three fingers (Maeda et al., 2020). The Kunitz peptides show much more adaptive binding strategies. For each target class, a distinct mode of action is used by these peptides. The mode of interaction of MQ1 to bind V2R is particularly efficient since MQ1 is the most selective V2R ligand so far described.

ACKNOWLEDGEMENTS

We thank Mathilde Gilles for her contribution in improving the quality of English language.

This work was supported by the French Atomic and Alternative Energies and *La Ligue contre le Cancer* for financial support and for the Amelia Chorfa PhD programme funding.

AUTHOR CONTRIBUTIONS

L.D., C.M., G.B., L.B., G.S., M.K., R.C.R.V., L.Q. and N.G. participated in research design. L.D., J.C., C.M., A.C., P.H., C.C., C.G., M.L., G.B., G.U., P.B., M.K., G.M., R.C.R.V. and L.Q. conducted experiments. L.D., G.B., G.M. and L.Q. contributed new reagents and analytic tools. L.D., C.M., G.B., M.K., R.C.R.V. and N.G. performed the data analysis. B.M., D.S., R.C.R.V., L.Q. and N.G. wrote or contributed to the writing of the manuscript.

CONFLICT OF INTEREST

No conflict of interest.

DECLARATION OF TRANSPARENCY AND SCIENTIFIC RIGOUR

This Declaration acknowledges that this paper adheres to the principles for transparent reporting and scientific rigour of preclinical research as stated in the *BJP* guidelines for **Natural Products Research, Design and Analysis**, and **Animal Experimentation**, and as recommended by funding agencies, publishers and other organizations engaged with supporting research.

DATA AVAILABILITY STATEMENT

The data that support the findings of this study are available from the corresponding author upon reasonable request.

ORCID

Servent Denis  <https://orcid.org/0000-0002-0774-1691>

REFERENCES

Ainsworth, S., Petras, D., Engmark, M., Süßmuth, R. D., Whiteley, G., Albuлесcu, L., Kazandjian, T. D., Wagstaff, S. C., Rowley, P., Wüster, W., Dorrestein, P. C., Arias, A. S., Gutiérrez, J. M.,

- Harrison, R. A., Casewell, N. R., & Calvete, J. J. (2018). The medical threat of mamba envenoming in sub-Saharan Africa revealed by genus-wide analysis of venom composition, toxicity and antivenomics profiling of available antivenoms. *Journal of Proteomics*, 172, 173–189. <https://doi.org/10.1016/j.jpro.2017.08.016>
- Andreev, Y., Kozlov, S. A., Koshelev, S. G., Ivanova, E. A., Monastyrnaya, M. M., Kozlovskaya, E. P., & Grishin, E. V. (2008). Analgesic compound from sea anemone *Heteractis crispata* is the first polypeptide inhibitor of vanilloid receptor 1 (TRPV1). *The Journal of Biological Chemistry*, 283, 23914–23921. <https://doi.org/10.1074/jbc.M800776200>
- Blanchet, G., Alili, D., Protte, A., Upert, G., Gilles, N., Tepshi, L., Stura, E. A., Mourier, G., & Servent, D. (2017). Ancestral protein resurrection and engineering opportunities of the mamba aminergic toxins. *Scientific Reports*, 7, 1–12. <https://doi.org/10.1038/s41598-017-02953-0>
- Blanchet, G., Collet, G., Mourier, G., Gilles, N., Fruchart-Gaillard, C., Marcon, E., & Servent, D. (2014). Polypharmacology profiles and phylogenetic analysis of three-finger toxins from mamba venom: Case of aminergic toxins. *Biochimie*, 103, 109–117. <https://doi.org/10.1016/j.biochi.2014.04.009>
- Bohlen, C. J., Chesler, A. T., Sharif-Naeini, R., Medzihradsky, K. F., Zhou, S., King, D., Sánchez, E. E., Burlingame, A. L., Basbaum, A. I., & Julius, D. (2011). A heteromeric Texas coral snake toxin targets acid-sensing ion channels to produce pain. *Nature*, 479, 410–414. <https://doi.org/10.1038/nature10607>
- Bourne, Y., Taylor, P., & Marchot, P. (1995). Acetylcholinesterase inhibition by fasciculins: Crystal structure of the complex. *Cell*, 83, 503–512. [https://doi.org/10.1016/0092-8674\(95\)90128-0](https://doi.org/10.1016/0092-8674(95)90128-0)
- Ciolek, J., Reinfrank, H., Quinton, L., Viengchareun, S., Stura, E. A., Vera, L., Sigismeau, S., Mouillac, B., Orce, H., Peigneur, S., Tytgat, J., Droctové, L., Beau, F., Nevoux, J., Lombès, M., Mourier, G., de Pauw, E., Servent, D., Mendre, C., ... Gilles, N. (2017). Green mamba peptide targets type-2 vasopressin receptor against polycystic kidney disease. *Proceedings of the National Academy of Sciences of the United States of America*, 114, 7154–7159. <https://doi.org/10.1073/pnas.1620454114>
- Cornett, L. E., & Dorsa, D. M. (1986). Regulation of (3H) arginine8 vasopressin binding to the rat renal medulla by guanine nucleotides. *Journal of Receptor Research*, 6, 127–140. <https://doi.org/10.3109/10799898609073928>
- Curtis, M. J., Alexander, S., Cirino, G., Docherty, J. R., George, C. H., Giembycz, M. A., Hoyer, D., Insel, P. A., Izzo, A. A., Ji, Y., MacEwan, D. J., Sobey, C. G., Stanford, S. C., Teixeira, M. M., Wonnacott, S., & Ahluwalia, A. (2018). Experimental design and analysis and their reporting II: Updated and simplified guidance for authors and peer reviewers. *British Journal of Pharmacology*, 175(7), 987–993. <https://doi.org/10.1111/bph.14153>
- Droctové, L., Lancien, M., Tran, V. L., Susset, M., Jegou, B., Theodoro, F., Kessler, P., Mourier, G., Robin, P., Diarra, S. S., Palea, S., Flahault, A., Chorfa, A., Corbani, M., Llorens-Cortes, C., Mouillac, B., Mendre, C., Pruvost, A., Servent, D., ... Gilles, N. (2020). A snake toxin as a theranostic agent for the type 2 vasopressin receptor. *Theranostics*, 10, 11580–11594. <https://doi.org/10.7150/thno.47485>
- Fruchart-Gaillard, C., Mourier, G., Blanchet, G., Vera, L., Gilles, N., Ménez, R., Marcon, E., Stura, E. A., & Servent, D. (2012). Engineering of three-finger fold toxins creates ligands with original pharmacological profiles for muscarinic and adrenergic receptors. *PLoS ONE*, 7, e39166. <https://doi.org/10.1371/journal.pone.0039166>
- Gasparini, S., Danse, J. M., Lecoq, A., Pinkasfeld, S., Zinn-Justin, S., Young, L. C., de Medeiros, C. C. L., Rowan, E. G., Harvey, A. L., & Ménez, A. (1998). Delineation of the functional site of α -dendrotoxin: The functional topographies of dendrotoxins are different but share a conserved core with those of other Kv1 potassium channel-blocking

- toxins. *The Journal of Biological Chemistry*, 273, 25393–25403. <https://doi.org/10.1074/jbc.273.39.25393>
- Harper, E., & Berger, A. (1967). On the size of the active site in proteases: I. Papain. *Biochemical and Biophysical Research Communications*, 27, 157–162.
- Harvey, A. L. (2001). Twenty years of dendrotoxins. *Toxicon*, 39, 15–26. [https://doi.org/10.1016/S0041-0101\(00\)00162-8](https://doi.org/10.1016/S0041-0101(00)00162-8)
- Huber, R., Kukla, D., Rühlmann, A., Epp, O., & Formanek, H. (1970). The basic trypsin inhibitor of bovine pancreas. I. Structure analysis and conformation of the polypeptide chain. *Naturwissenschaften*, 57, 389–392. <https://doi.org/10.1007/BF00599976>
- Izzo, A. A., Teixeira, M., Alexander, S. P., Cirino, G., Docherty, J. R., George, C. H., Insel, P. A., Ji, Y., Kendall, D. A., Panattieri, R. A., Sobey, C. G., Stanford, S. C., Stefanska, B., Stephens, G., & Ahluwalia, A. (2020). A practical guide for transparent reporting of research on natural products in the British Journal of Pharmacology: Reproducibility of natural product research. *British Journal of Pharmacology*, 177(10), 2169–2178. <https://doi.org/10.1111/bph.15054>
- Juul, K. V., Bichet, D. G., Nielsen, S., & Nørgaard, J. P. (2014). The physiological and pathophysiological functions of renal and extrarenal vasopressin V2 receptors. *American Journal of Physiology. Renal Physiology*, 306, F931–F940. <https://doi.org/10.1152/ajprenal.00604.2013>
- Kawamura, K., Yamada, T., Kurihara, K., Tamada, T., Kuroki, R., Tanaka, I., Takahashi, H., & Niimura, N. (2011). X-ray and neutron protein crystallographic analysis of the trypsin-BPTI complex. *Acta Crystallographica. Section D, Biological Crystallography*, 67, 140–148. <https://doi.org/10.1107/S0907444910053382>
- Kessler, P., Marchot, P., Silva, M., & Servent, D. (2017). The three-finger toxin fold: A multifunctional structural scaffold able to modulate cholinergic functions. *Journal of Neurochemistry*, 142(Suppl), 7–18. <https://doi.org/10.1111/jnc.13975>
- Kunitz, M., & Northrop, J. H. (1936). Isolation from beef pancreas of crystalline trypsinogen, trypsin, a trypsin inhibitor, and an inhibitor-trypsin compound. *The Journal of General Physiology*, 19, 991–1007. <https://doi.org/10.1085/jgp.19.6.991>
- Lilley, E., Stanford, S. C., Kendall, D. E., Alexander, S. P., Cirino, G., Docherty, J. R., George, C. H., Insel, P. A., Izzo, A. A., Ji, Y., Panattieri, R. A., Sobey, C. G., Stefanska, B., Stephens, G., Teixeira, M., & Ahluwalia, A. (2020). ARRIVE 2.0 and the *British Journal of Pharmacology*: Updated guidance for 2020. *British Journal of Pharmacology*, 177(16), 3611–3616. <https://doi.org/10.1111/bph.15178>
- Maeda, S., Xu, J., N. Kadji, F. M., Clark, M. J., Zhao, J., Tsutsumi, N., Aoki, J., Sunahara, R. K., Inoue, A., Garcia, K. C., & Kobilka, B. K. (2020). Structure and selectivity engineering of the M1 muscarinic receptor toxin complex. *Science*, 369, 161–167. <https://doi.org/10.1126/science.aax2517>
- Maïga, A., Mourier, G., Quinton, L., Rouget, C., Gales, C., Denis, C., Lluell, P., Sénard, J. M., Palea, S., Servent, D., & Gilles, N. (2012). G protein-coupled receptors, an unexploited animal toxin targets: Exploration of green mamba venom for novel drug candidates active against adrenoceptors. *Toxicon*, 59, 487–496. <https://doi.org/10.1016/j.toxicon.2011.03.009>
- Otlewski, J., Jaskólski, M., Buczek, O., Cierpicki, T., Czapinska, H., Krowarsch, D., Smalas, A. O., Stachowiak, D., Szpineta, A., & Dadlez, M. (2001). Structure-function relationship of serine protease-protein inhibitor interaction. *Acta Biochimica Polonica*, 48, 419–428. https://doi.org/10.18388/abp.2001_3926
- Percie du Sert, N., Hurst, V., Ahluwalia, A., Alam, S., Avey, M. T., Baker, M., Browne, W. J., Clark, A., Cuthill, I. C., Dirnagl, U., Emerson, M., Garner, P., Holgate, S. T., Howells, D. W., Karp, N. A., Lazic, S. E., Lidster, K., MacCallum, C. J., Macleod, M., ... Würbel, H. (2020). The ARRIVE guidelines 2.0: Updated guidelines for reporting animal research. *PLoS Biology*, 18(7), e3000410. <https://doi.org/10.1371/journal.pbio.3000410>
- Quinton, L., Girard, E., Maïga, A., Rekik, M., Lluell, P., Masuyer, G., Larregola, M., Marquer, C., Ciolek, J., Magnin, T., Wagner, R., Molgó, J., Thai, R., Fruchart-Gaillard, C., Mourier, G., Chamot-Rooke, J., Ménez, A., Palea, S., Servent, D., & Gilles, N. (2010). Isolation and pharmacological characterization of AdTx1, a natural peptide displaying specific insurmountable antagonism of the α_{1A} -adrenoceptor. *British Journal of Pharmacology*, 159, 316–325. <https://doi.org/10.1111/j.1476-5381.2009.00532.x>
- Rouget, C., Quinton, L., Maïga, A., Gales, C., Masuyer, G., Malosse, C., Chamot-Rooke, J., Thai, R., Mourier, G., de Pauw, E., Gilles, N., & Servent, D. (2010). Identification of a novel snake peptide toxin displaying high affinity and antagonist behaviour for the α_2 -adrenoceptors. *British Journal of Pharmacology*, 161, 1361–1374. <https://doi.org/10.1111/j.1476-5381.2010.00966.x>
- Schweitz, H., Heurteaux, C., Bois, P., Moinier, D., Romey, G., & Lazdunski, M. (1994). Calciudine, a venom peptide of the Kunitz-type protease inhibitor family, is a potent blocker of high-threshold Ca^{2+} channels with a high affinity for L-type channels in cerebellar granule neurons. *Proceedings of the National Academy of Sciences*, 91, 878–882. <https://doi.org/10.1073/pnas.91.3.878>
- Shafqat, J., Zaidi, Z. H., & Jörnvall, H. (1990). Purification and characterization of a chymotrypsin Kunitz inhibitor type of polypeptide from the venom of cobra (*Naja naja naja*). *FEBS Letters*, 275, 6–8. [https://doi.org/10.1016/0014-5793\(90\)81426-O](https://doi.org/10.1016/0014-5793(90)81426-O)
- Strydom, D. J., & Joubert, F. J. (1981). The amino acid sequence of a weak trypsin inhibitor B from *Dendroaspis polylepis polylepis* (black mamba) venom. *Hoppe-Seyler's Zeitschrift für Physiologische Chemie*, 362, 1377–1384. <https://doi.org/10.1515/bchm2.1981.362.2.1377>
- Sun, D., Yu, Y., Xue, X., Pan, M., Wen, M., Li, S., Qu, Q., Li, X., Zhang, L., Li, X., Liu, L., Yang, M., & Tian, C. (2018). Cryo-EM structure of the ASIC1a-mambalgin-1 complex reveals that the peptide toxin mambalgin-1 inhibits acid-sensing ion channels through an unusual allosteric effect. *Cell Discovery*, 4, 1–11. <https://doi.org/10.1038/s41421-018-0026-1>
- Zhou, X. D., Jin, Y., Lu, Q. M., Li, D. S., Zhu, S. W., Wang, W. Y., & Xiong, Y. L. (2004). Purification, characterization and primary structure of a chymotrypsin inhibitor from *Naja atra* venom. *Comparative Biochemistry and Physiology Part B: Biochemistry and Molecular Biology*, 137, 219–224. <https://doi.org/10.1016/j.cbpc.2003.11.007>

SUPPORTING INFORMATION

Additional supporting information may be found in the online version of the article at the publisher's website.

How to cite this article: Droctové, L., Ciolek, J., Mendre, C., Chorfa, A., Huerta, P., Carvalho, C., Guin, C., Lancien, M., Stanajic-Petrovic, G., Braco, L., Blanchet, G., Upert, G., De Pauw, G., Barbe, P., Keck, M., Mourier, G., Mouillac, B., Denis, S., Rodríguez de la Vega, R. C., ... Gilles, N. (2022). A new Kunitz-type snake toxin family associated with an original mode of interaction with the vasopressin 2 receptor. *British Journal of Pharmacology*, 179(13), 3470–3481. <https://doi.org/10.1111/bph.15814>